Research Article

Nano-Carbonated Hydroxyapatite from Bovine Bone Combined With Platelet-Rich Plasma Accelerates Fracture Healing in *Rattus norvegicus* Models

Zahra Jamilah Sabrina[1], Adrian Pearl Gunawan[2], Beryl Reinaldo Chandra[2], Ilham Pangestu Harwoko[3], Johannes Marulitua Nainggolan[4], Widi Nugroho[1*]

[1]Laboratory of Veterinary Public Health, Faculty of Veterinary Medicine, Universitas Brawijaya, Malang, Indonesia; [2]Faculty of Medicine, Universitas Brawijaya, Malang, Indonesia; [3]Department of Biology, Faculty of Mathematics and Natural Sciences, Universitas Brawijaya, Malang, Indonesia; [4]Department of Physics, Faculty of Mathematics and Natural Sciences, Universitas Brawijaya, Malang, Indonesia.

Abstract | Fracture causes physical disability, psychological stress or even fatal to a patient. Autograft and allograft have long been used to improve fracture healing, but flaws limit their use. Xenograft from micro-carbonated hydroxyapatite (micro-CHA) and nano-CHA from bovine bone combined with Platelet-Rich Plasma (PRP) was hypothesized to accelerate fracture healing. This study aimed to characterise micro-CHA and nano-CHA synthesized from bovine bone and analyze their effects as xenografts on fracture healing in *Rattus norvegicus* models. The micro-CHA was synthesized using thermal treatment at 720°C, and nano-CHA was made from the micro-CHA using nano-milling. The PRP was isolated from each rat. Twenty four rats were fractured at the right tibial bones and divided into four groups; control, micro-CHA, micro-CHA+PRP, and nano-CHA+PRP treatments. Characteristics of micro-CHA and nano-CHA were analysed using Particle Size Analyser (PSA), Fourier Transform Infrared Spectroscopy (FTIR), XRD (X-Ray Diffraction) and Scanning Electron Microscope (SEM). The course of fracture healings was analysed at 21 days post-treatment using Emery's score and Kruskal-Wallis and Mann Whitney U statistics. Results showed that micro-CHA has a molecular formula of $Ca_{10}(PO_4)_3(CO_3)_5(OH)$ and a crystallinity level of 89.97%. Nano-CHA has agglomerate sizes of 82.68 – 153.00 nm. Emery's score in the nano-CHA+PRP group was highest amongst all groups (P<0.05). Emery's score in the micro-CHA+PRP group was higher than that in the micro-CHA and control groups (P<0.05). Emery's scores in the control and micro-CHA groups were similar (P>0.05). This study suggests that PRP-supplemented nano-CHA from bovine bone could accelerate fracture healing in rat models.

Keywords | Bone graft, Xenograft, Nano-carbonated hydroxyapatite, Platelet Rich Plasma, Fracture

Received | March 16, 2022; **Accepted** | April 30, 2022; **Published** | June 01, 2022
***Correspondence** | Widi Nugroho, Laboratory of Veterinary Public Health, Faculty of Veterinary Medicine, Universitas Brawijaya, Malang, Indonesia; **Email:** widi.nugroho@ub.ac.id
Citation | Sabrina ZJ, Gunawan AP, Chandra BR, Harwoko IP, Nainggolan JM, Nugroho W (2022). Nano-carbonated hydroxyapatite from bovine bone combined with platelet-rich plasma accelerates fracture healing in *rattus norvegicus* models. Adv. Anim. Vet. Sci. 10(6): 1296-1302.
DOI | http://dx.doi.org/10.17582/journal.aavs/2022/10.6.1296.1302
ISSN (Online) | 2307-8316

INTRODUCTION

As many as 178 million cases of fractures occurred in the human population worldwide in 2019 (Wu et al., 2021). The most common fracture is a hip fracture, and it is predicted to affect 4.5 million people globally in 2050 (Veronese and Maggi, 2018). Fractures can cause various complications, from local abnormality to life-threatening

ischemia (Blom et al., 2018). Fracture patients would be dependent on others even for basic needs, thus reducing the productivity of the affected community.

Fractures in animals are not as massive as that in humans, but incidences are reported worldwide and continuously occur. In the US, 175 fractures in cats were reported during 2018 (Reyes et al., 2019). In Southeast Queensland, Australia, there were 2031 fracture cases in wild koalas from 1997 to 2010 (Henning et al., 2014). In Libya, there were 650 cases of fractures in dogs (67%) and cats (23%) during the period from 2005 to 2010 (Ben Ali, 2013). Between 2011 and 2013, in India, there were 206 cases of fractures in various animal species, including dogs, goats, cats, poultry, rabbits, cattle, and monkeys (Singh et al., 2017). Fracture in animals is generally an animal welfare issue, but it is also a productivity issue in working and breeding animals. Medical treatments of fractures can be performed by bone grafts (Blom et al., 2018). It promotes bone healing through osteogenesis, osteoinduction and osteoconduction (Shibuya and Jupiter, 2015). One primary method of bone grafting is autograft, which is implanting tissues from other parts of the same individual to fracture area. It has disadvantages such as pain, morbidity at the site of the donor organ, limited availability, the need for further surgery, hematoma, infection, the need for sedation or general anaesthesia, longer operation time duration, and blood loss (Oryan et al., 2014). An alternative to the autograft method is the allograft, performed by taking implants from another individual in the same species. It has numerous disadvantages, such as the lack of osteogenicity, the risk of disease transmission, varied osteoinductivity, limited availability, and restriction in some countries for ethical consideration (Oryan et al., 2014). Due to these limitations, an alternative bone graft with excellent osteoinductivity and conductivity yet, low in cost but highly available, is needed. The other method of bone grafting is the xenograft, i.e. a bone grafting that uses material from other species as an implant. Several xenograft sources have been investigated and proven to have potential as an alternative to improve fracture healing, such as carbonated hydroxyapatite (CHA) and tri calcium phosphate (Hosseinzadeh et al., 2014).

Studies have shown that the osteoconductive and biocompatible properties of CHA can be improved by reducing the particle size of CHA from micro to nano-level. Nano-CHA has a larger total surface area than the same weight of micro-CHA (Karunakaran et al., 2019), and is more osteologically conductive and more biologically compatible than micro-CHA (Dhanalakshmi et al., 2012; Mavropoulos et al., 2012). In vivo studies showed that nano-CHA have a better receptive response by animals than micro CHA (Calasans-Maia et al., 2015). Carbonated hydroxyapatite (CHA) xenografts from bovine bones have been reported to have better performance than snail shells, plants and algae due to a high calcium carbonate content (Asimeng et al., 2020). Further, the PRP is also known to improve tissue healing in animal models (Moradi et al., 2015; Rodriguez et al., 2014). However, the potential of nano-xenograft made from bovine bone enriched with PRP to accelerate fracture healing in vertebrates is still open for investigation.

This research aimed to synthesize and characterize micro-CHA and nano-CHA from bovine bone and investigate the effect of the micro-CHA and nano-CHA supplemented with platelet-rich plasma (PRP) as xenografts to stimulate osteogenesis and improve the fracture healing process in *Rattus norvegicus* models.

MATERIAL AND METHODS

Ethical consideration location of the study

This study was approved by the Committee of Animal Care and Use of Universitas Brawijaya No. 055-KEP-UB-2021. Animals were maintained at the animal care facility of faculty of Veterinary Medicine, Universitas Brawijaya. Synthesis of micro-CHA and nano-CHA was performed at Laboratory of Physics, Faculty of Sciences, Universitas Brawijaya. The PSA and FTIR analyses of nano-CHA was performed at Laboratory of Chemistry, Faculty of Sciences, Universitas Brawijaya. The analyses of SEM and EDS were performed at the Laboratorium Sentra Ilmu Hayati, Universitas Brawijaya. The PRP preparation and surgery was performed at the laboratory of Veterinary Surgery, Veterinary Medicine, Universitas Brawijaya. Histopathological preparation and analysis were conducted at Laboratory of Pathology and Anatomy, Universitas Islam Malang.

Synthesis of the micro-CHA and nano-CHA

The adult bovine femur was cut into small pieces and cleaned from soft tissue, periosteum, and bone marrow. The bone was further crushed into powder and sieved using 200 mesh filters (74 µm). The bone powder was soaked in chloroform for 6 hours, washed and rinsed three times using distilled water and dried in an oven for 15 minutes at 150°C. Subsequently, it was soaked in acetone for 2 hours and rinsed three times with distilled water, then was dried in an oven at 170°C for 24 hours. CHA was sinthesised from the bone powder by thermal decomposition, through heating the powder in an alumina container at 750°C for 6 hours (Hosseinzadeh et al., 2014) . The CHA was sieved through a 325 mesh filter to obtain 44 µm size micro-CHA particles. In order to produce particles of nano-CHA, the micro-CHA powder was put into a ball miller and rotated at 400 rpm for 2 hours (Esmaeilkhanian et al., 2019). The process was repeated two times. The mass ratio of the ball

to the micro CHA powder was 10 in the first milling and the ratio was increased to 20 during the second milling. The nano-CHA formed was stored in a sterile container at room temperature for further characterisation.

Characterisations of the micro-CHA and nano-CHA

The Particle Size Analyser (PSA, Type 1090/Cilas, California, US) was used to analyse the particle size distribution of the micro-CHA powder. Fourier Transform Infrared Spectroscopy (FTIR) (IRSpirit/ATR-S Serial No. A224158/Shimadzu, Kyoto, Japan) was used to analyse the functional group of the micro-CHA molecule. The phase, molecular formula and crystallinity of the nano-CHA were characterised using an X-Ray Diffractometer (XRD) (Malvern Panalytical, Eindhoven, Netherlands) assisted by Highscore-plus software (Malvern Panalytical, Worcestershire, UK). Surface morphology, size and elements of nano-CHA particle were analysed using a scanning electron microscope (SEM) (FEI - Quanta 650 FEG SEM, Abingdon, Oxfordshire, UK), equipped with energy dispersive spectroscopy (EDS) (AZtecOne/X-act, Abingdon, Oxfordshire, UK).

Preparation of Platelet-Rich Plasma (PRP)

The rat was bled, and two millimetres of blood was collected in an EDTA tube. Blood was centrifuged at 3000 rpm for 10 minutes, the plasma was extracted and centrifuged at 3000 rpm for 10 minutes to precipitate the platelet. The precipitate (the PRP), was taken using micropipette and immediately added to micro-CHA or nano-CHA.

The preparation of CHA Paste+PRP

To make the paste of micro-CHA or nano-CHA, the respective CHA was added to 10% (w/v) of PEG in 2-propanolol, with the mass ratio of micro-CHA or nano-CHA to PEG was two. To make the CHA+PRP, the micro-CHA or nano-CHA was added to 0.2 mL to the concentration of PRP in CHA paste of 40% (w/w). The CHA+PRP was immediately applied to fractures after the mixing.

Bone fracture formation and paste administration

A total of 24 Wistar rats (*Rattus norvegicus*) with a mean weight of 188.5 g (range: 130.0 - 281.0 g) were used in the study. After a week of acclimatisation, the animals were randomly allocated into four groups based on different treatments: A, control; B, micro-CHA treatment; C, micro-CHA+PRP treatment and; D. Nano-CHA+PRP treatment.

To develop fracture models, the rats were anaesthetised using ketamine HCl (90 mg/kg, 100 mg/mL, IM) and xylazine (12 mg/kg, 20 mg/mL, IM). The rats were given IM prophylactic antibiotic ceftriaxone (30 mg/kg), 70 mg/mL in 0.5% lidocaine). Under anaesthesia, the skin of the right tibia of the rat was shaved and decontaminated with 70% alcohol and with 10% povidone-iodine. The skin of the diaphysis of the right tibia was incised craniocaudally from ±0.5 cm distance of the tibiofemoral joint to the direction of tibio-tarsal joint, one cm in length, with a surgical blade number 22. The skin and fascia were extended laterally to expose the tibial bone. The fracture model was made by cutting the diaphysis of tibial bones at a 45° angle in both directions at one mm depth thus, forming a triangle-shaped of the discontinued bone area in the tibia. The blood was cleaned with sterile cotton, the surgical site was moistened with 0.9% NaCl. After the fracture was made, 0.02 g of micro-CHA, micro-CHA+PRP or, the nano-CHA+PRP paste was applied at the fractured site. Subsequently, the fascia and skin were sutured with sterile 3/0 catgut. The surgical site was cleaned with 0.9% NaCl, 70% alcohol in cotton and 10% povidone-iodine. Rats were given Meloxicam 0.01 mL IM as an analgesic and the wound was bandaged.

Histopathological preparation

The animals were euthanised at 21 days after surgery by cervical dislocation (Mondal et al., 2012). The tibial bones of the rats were cut at 0.5 cm cranial and 0.5 cm caudal from the fractured area. The cut bones were labelled and soaked in a 10% formalin buffer and treated with a decalcifying agent for 10 minutes (Rolls, 2010). Samples were then embedded into the paraffin and cut using a rotary microtome at the thickness of 0.4 mm at the central aspects of the bone sample, and stained with the Hematoxylin & Eosin.

Statistical Analysis

The histopathological analysis was performed using Emery's histopathological criteria with the score ranges 0 – 7. Briefly, score 0 represents empty cavity, score 1 represents the presence of fibrous tissue only; score 2 represents the presence of more fibrous tissue than fibrocartilage; score 3 represents the presence of more fibrocartilage than fibrous tissue; score 4 represents the presence of fibrocartilage only; score 5 represents the presence of more fibrocartilage than bone matrix; score 6 represents the presence of more bone matrix than fibrocartilage and score 7 represents the presence of bone matrix only (Mondal et al., 2012). The scores were further analysed using Kruskal-Wallis and Mann Whitney U statistics, at a significant level of $P<0.05$. Statistical calculations were done using SPSS version 20 software (SPSS, Chicago, IL, USA).

RESULTS

Characteristics of micro-CHA and nano-CHA

The PSA characterisation showed that the mean size of micro-CHA powder prior to nano-milling was 39.98 µm (SD: 4.21 - 80.97 µm) (Figure 1a). FTIR analysis of the micro-CHA powder showed that it contained functional groups of OH^-, CO_3^{2-} and PO_4^{3-} which were the main components of the CHA molecule. The CO_3^{2-} group was detected between the wavelength of 1.411 cm^{-1} and 1.461 cm^{-1}. The OH^- group was detected within the wavelength of 3.437 cm^{-1} and 3.572 cm^{-1}. The PO_4^{3-} group was detected within the wavelength of 1.042 cm^{-1} and 1.093 cm^{-1} (Figure 1b). The XRD analysis showed that the micro-CHA contained carbonated hydroxyapatite with a complex formula of $Ca_{10}(PO_4)_3(CO_3)_5(OH)$ with a hexagonal crystalline formation. The nano-CHA had a crystallinity of 89.97%, with the prominent diffraction peaks formed at the diffraction angle of 31.74° (Figure 1c). The elements in nano-CHA materials had a weight ratio of C (14.76%), O (60%), P (9.64%), Ca (14.45%), Mg (0.54%) and Na (0.56%).

The nano-milling process reduced the size of micro-CHA into nanoparticles, as shown by the SEM analysis at the magnification of 10,000x (Figure 1d). The shape of the particles was spherical and a few particles were joining together to form agglomerates. The size of agglomerates ranging from 82.68 - 153 nm.

Histopathological Analysis

In the treatment group with nano-CHA+PRP, woven bone tissue dominated the fracture area, indicating the bones were in the remodelling phase. The group of micro-CHA+PRP were in the stage of hard callus formation characterised by the domination of fibrocartilage tissue and the presence of a small proportion of woven bones. The group of micro-CHA was in the late phase of soft callus formation, which was characterised by the domination of fibrocartilage tissue and chondrocytes. The bone healing process of the control group was in the early phase of soft callus formation, which was characterised by the domination of fibrous tissue and the presence of a small proportion of fibrocartilage tissue (Figure 2).

Further statistical analyses on Emery's score of fracture healing using Kruskal-Wallis test indicated significant difference among groups (P=0.0003). The Mann Whitney U follow-up test showed that the nano-CHA+PRP group had the highest Emery's score amongst all groups (P<0.05). The Emery's scores between the control and micro-CHA groups were not significantly different (P>0.05), but the Emery's score of the micro-CHA+PRP group was higher than that of the micro-CHA and control groups (P<0.05).

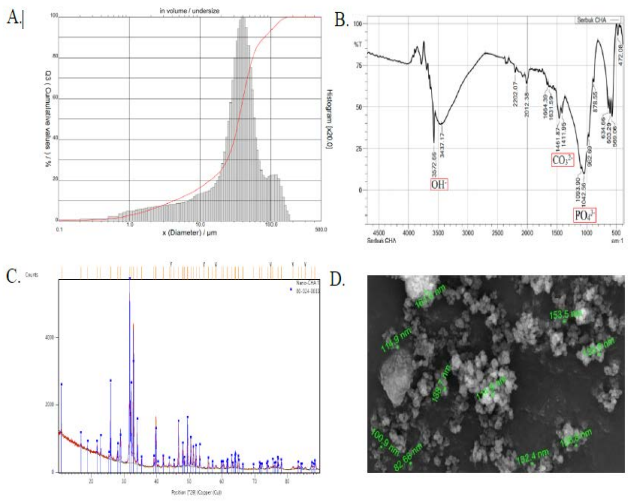

Figure 1: Characteristics of CHA; A. Particle size distribution of micro-CHA analyzed using PSA; the mean size of the particles is 39.98 µm (SD: 4.21 - 80.97 µm); B. The FTIR analysis of micro-CHA shows functional groups of OH-, CO32- and PO43-; C. The XRD analysis of nano-CHA shows the prominent diffraction peaks formed at the diffraction angle of 31.74°; D. The particle size distribution of nano-CHA analyzed using SEM at 10.000x magnification; the particles were of spherical shapes, a few particles were joining together to form agglomerates with the size of agglomerates ranging 82.68 - 153 nm.

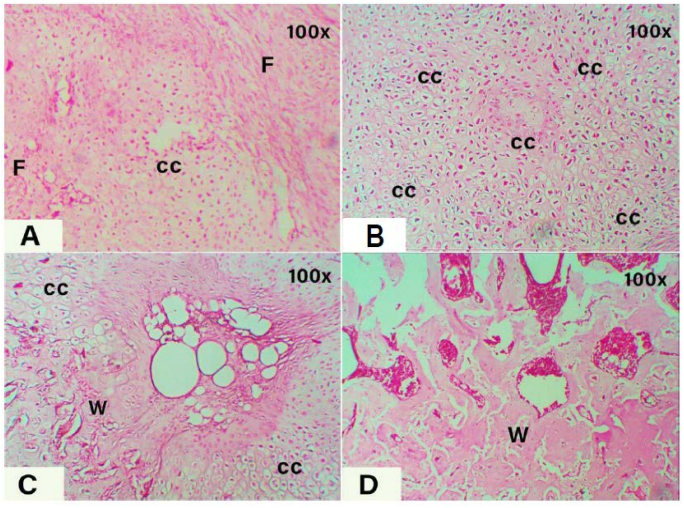

Figure 2: Sections of fractured tibial bone tissues at 21 days post-treatments. A. control group, showing the formation of fibrocartilage tissue by chondrocyte cells (cc) in between the fibrous tissue (F) which was developed earlier; B. Micro-CHA group showing the complete formation of fibrocartilage tissue (Fc) indicates the late phase of soft callus formation; C. Micro-CHA+PRP group, showing the domination of fibrocartilage tissue and the formation of a small proportion of woven bone tissue (W) indicating a hard callus formation; D. Nano-CHA+PRP group,

showing the formation of new bone matrix in the fractured area indicated by the domination of woven bone and fusion into lamellar bone. H&E staining, 100x magnification.

DISCUSSION

This study reported the synthesis and application of nano-CHA from bovine bone to accelerate tissue healing in the animal model. The CHA from bovine bone produced by thermal decomposition has a higher percentage of crystallinity as the heating temperature increases. It was shown by the higher intensity and narrower peak width in the XRD analysis. The functional groups of the CHA produced in this study were in accordance with the previous studies, which reported that the phosphate group of the CHA was detected at the wavelength of ~1,000 cm^{-1}, the carbonate group was at the wavelength of ~1,400 cm^{-1} and the hydroxyl group was at the wavelength of ~3,300 cm^{-1} (Venkatesan and Kim, 2010; Mondal et al., 2012). Nano-CHA produced in the current study may represent characteristics of B-type CHA. The B-type CHA contained CO_3^{2-} at ~1465 cm^{-1} (CO_3 substitutes for PO_4), while A-type CHA contained CO_3^{2-} at ~1546 cm^{-1} (CO_3 substitutes for OH) (Ren and Leng, 2011). The ratio of Ca to P in CHA of the current study was 1.5, similar to that in cancellous bone of young bovine (Kuhn et al., 2008).

In this study, the nano-CHA appeared to capable of enhancing the fractur healing in animal models, compared to that in micro-CHA treated group. Within three weeks, the fractured area of animal models in nano-CHA+PRP group had developed into the final fracture healing process of remodelling phase, while in micro-CHA+PRP treated group, the process developed slower and only reached hard callus formation phase. Similarly, another study in rat models indicated that the bone healing process in a nano-CHA implanted fracture was faster than the bone healing process in micro-CHA implanted fracture (Pascawinata et al., 2018). A study in rabbits reported that complete callus formation in fracture injury had started on as soon as day 30 post treatment in the nano-CHA treated group, while in the group without treatment, it was only started on day 60 post fracture (Rahimzadeh et al., 2012). The synthesis of CHA from animal bones using thermal decomposition seems to produce CHA which not only smaller in size which facilitate a better uptake by vetrebrate tissue in-vivo, but also is free from antigenic organic material, that make it compatible for use in in-vivo bone tissue reparation c. Further, the strength of hydroxyapatite xenograft was a similar to that of cortical allografts but greater than that of cancellous allografts (Hosseinzadeh et al., 2014). Application of nanoscale materials in skeletal tissue regeneration has a potential to replace the existing technology of orthopaedic reparations (Yi et al., 2016).

In addition to nano-CHA, in current study, the PRP apparently played a role to accelerate bone healing. The micro-CHA+PRP treatment showed a significant acceleration of fracture healing compared to that in micro-CHA group without supplementation of PRP. Previous study in rat models indicated that the application of PRP to the fracture site significantly improved fracture healing and enhanced the biomechanical strength of the fractured joint (Moradi et al., 2015). The PRP contains ample growth factors such as platelet-derived growth factor, epidermal growth factor, fibroblast growth factor, transforming growth factor-β, vascular endothelial growth factor, as well as tissue healing factors such as IL-1, IL-6, TNF-α, fibronectin, vitronectin and IGF which play significant roles in bone remodelling process (Rodriguez et al., 2014).

However, the current study did not include the nano-CHA group without the supplementation of PRP. Thus, while nano-CHA+PRP was shown to accelerate fracture healing compared to micro-CHA+PRP, it remains unclear how the nano-CHA without PRP accelerates fracture healing compared to nano-CHA+PRP and micro-CHA+PRP and warrants further study.

CONCLUSION

The findings of this study suggest that the application of nano-CHA+PRP to experimental fracture could accelerate fracture healing in rat models among different treatment groups. Further research is needed to confirm the potential of nano-CHA+PRP from bovine bone to accelerate fracture healing in other species and humans.

ACKNOWLEDGEMENTS

The research was funded by the Ministry of Education and Culture Republic of Indonesia with grant number: 1949/E2/KM.05.01/2021. We thank drh. Muhamad Arfan Lesmana, M.Sc. and drh. Dian Vidiastuti, M.Sc. for supervision during animal surgery. We also thank Nike Fitayatul Khusnah, S.Si., for assistance during XRD and SEM analyses and Mohammad Farid Rahman, S.Si., M.Si. for assistance during PSA and FTIR analyses. We thank Wike Astrid Cahyani, S.Ked, M.Biomed. for supervision during histopathological analysis

CONFLICT OF INTEREST

The authors declare that there is no conflict of interest in regard with the publication of this manuscript.

AUTHOR CONTRIBUTIONS

Conseptualisation: Zahra Jamilah Sabrina, Adrian Pearl

Gunawan, Beryl Reinaldo Chandra, Ilham Pangestu Harwoko, Johannes Marulitua Nainggolan and Widi Nugroho. **Data collection and management:** Zahra Jamilah Sabrina and Johannes Marulitua Nainggolan. **Formal analysis:** Adrian Pearl Gunawan, Beryl Reinaldo Chandra, and Ilham Pangestu Harwoko. **Writing-draft, review and approval of the manuscript:** Zahra Jamilah Sabrina, Adrian Pearl Gunawan, Beryl Reinaldo Chandra, Ilham Pangestu Harwoko, Johannes Marulitua Nainggolan and Widi Nugroho.

REFERENCES

Asimeng OB, Walter Afeke D, Kwason Tiburu E. (2020). Biomaterial for Bone and Dental Implants: Synthesis of B-Type Carbonated Hydroxyapatite from Biogenic Source. In Biomaterials. 121–130. https://doi.org/10.5772/intechopen.92256

Ben Ali LM (2013). Incidence, Occurrence, Classification and Outcome of Small Animal Fractures: A Retrospective Study (2005-2010). World Acad. Sci., Engineer. Technol. Int. J. Anim. Vet. Sci. 7(3): 191–196. https://doi.org/14106/incidence-occurrence-classification-and-outcome-of-small-animal-fractures-a-retrospective-study-2005-2010-.

Blom Ashley, Warwick David, Whitehouse, Michael NB (2018). Apley and Solomon's System of Orthopaedics and Trauma (D. Warwick, Ed.; Tenth). 6000 Broken Sound Parkway NW, Suite 300 Boca Raton, FL 33487-2742: CRC Press.

Calasans-Maia M, de Melo B, Alves A., Resende R., Louro R., Sartoretto S., Granjeiro J, Alves G. (2015). Cytocompatibility and biocompatibility of nanostructured carbonated hydroxyapatite spheres for bone repair. J. Appl. Oral Sci. 23(6): 599–608. https://doi.org/10.1590/1678-775720150122

Cavalu S, Antoniac IV, Mohan A, Bodog F, Doicin C, Mates I, Ulmeanu M, Murzac R, Semenescu A (2020). Nanoparticles and nanostructured surface fabrication for innovative cranial and maxillofacial surgery. Materials. 13(23): 1–23. https://doi.org/10.3390/ma13235391

Dhanalakshmi CP, Vijayalakshmi L, Narayanan V (2012). Nanocomposites of Carbonated Hydroxyapatite/Poly (4-vinyl pyridine-co-styrene): Synthesis, Characterization and its Application. Nano Hybrids. *2*: 65–85. https://doi.org/10.4028/www.scientific.net/nh.2.65

Esmaeilkhanian A., Sharifianjazi F., Abouchenari A., Rouhani A., Parvin N., Irani M. (2019). Synthesis and Characterization of Natural Nano-hydroxyapatite Derived from Turkey Femur-Bone Waste. Appl. Biochem. Biotechnol. 189(3): 919–932. https://doi.org/10.1007/s12010-019-03046-6.

Henning J, Hannon C, McKinnon A, Larkin R, Allavena R (2014). The causes and prognoses of different types of fractures in wild koalas submitted to wildlife hospitals. Prevent. Vet. Med. 122(3): 371–378. https://doi.org/10.1016/j.prevetmed.2015.10.015

Hosseinzadeh E, Davarpanah M, Nemati NH, Tavakoli SA (2014). Fabrication of a hard tissue replacement using natural hydroxyapatite derived from bovine bones by thermal decomposition method. Int. J. Organ Transplantat. Med. 5(1): 23–31.

Karunakaran G., Kumar G., Cho E., Sunwoo Y., Kolesnikov E., and Kuznetsov D. (2019) Microwave-assisted hydrothermal synthesis of mesoporous carbonated hydroxyapatite with tunable nanoscale characteristics for biomedical applications. Ceram. Int. *45*(1): 970–977. https://doi.org/10.1016/j.ceramint.2018.09.273.

Kuhn LT, Grynpas MD, Rey CC, Wu Y, Ackerman JL, Glimcher MJ (2008). A Comparison of the Physical and Chemical Differences Between Cancellous and Cortical Bovine Bone Mineral at Two Ages. Calcified Tissue Int. 83(2): 146–154. https://doi.org/10.1007/s00223-008-9164-z

Mavropoulos E., Hausen M., Costa A., Albuquerque S., Alves G., Granjeiro J., Rossi A (2012). Biocompatibility of carbonated hydroxyapatite nanoparticles with different crystallinities. Key Engin. Mat. 493: 331–336. https://doi.org/10.4028/www.scientific.net/KEM.493-494.331

Mondal S., Mondal B., Dey A., Mukhopadhyay SS (2012). Studies on Processing and Characterization of Hydroxyapatite Biomaterials from Different Bio Wastes. J. Minerals Mat. Characterizat. Engin. 11(1): 55–67. https://doi.org/10.4236/jmmce.2012.111005

Moradi AH, Kamalinejad A, Jalilian N, Kazemi S, Khazaei M (2015). Using PRP and human amniotic fluid combination for osteogenesis in rabbit socket preservation. Dental Hypotheses. *6*(4): 151–155. https://doi.org/10.4103/2155-8213.170642

Oryan A., Alidadi S., Moshiri A., Maffulli N. (2014). Bone regenerative medicine: Classic options, novel strategies, and future directions. J. Orthopaed. Surg. Res. 9(1): 1–27. https://doi.org/10.1186/1749-799X-9-18

Pascawinata A, Prihartiningsih P, Dwirahardjo B. (2018). Perbandingan proses penyembuhan tulang antara implantasi hidroksiapatit nanokristalin dan hidroksiapatit mikrokristalin, kajian pada tulang tibia kelinci. B-Dent, Jurnal Kedokteran Gigi Universitas Baiturrahmah. *1*(1): 1–10. https://doi.org/10.33854/jbdjbd.45

Rahimzadeh R, Veshkini A, Sharifi D, Hesaraki S (2012). Value of color Doppler ultrasonography and radiography for the assessment of the cancellous bone scaffold coated with nano-hydroxyapatite in repair of radial bone in rabbit. Acta Cirurgica Brasileira. *27*(2): 148–154. https://doi.org/10.1590/s0102-86502012000200009

Ren FZ, Leng Y (2011). Carbonated Apatite, Type-A or Type-B. Key Engineer. Mat. 493: 293–297. https://doi.org/10.4028/www.scientific.net/KEM.493-494.293

Reyes NA, Longley M, Bailey S, Langley-Hobbs SJ (2019). Incidence and types of preceding and subsequent fractures in cats with patellar fracture and dental anomaly syndrome. J. Feline Med. Surg. 21(8): 750–764. https://doi.org/10.1177/1098612X18800837

Rodriguez IA., Growney Kalaf EA., Bowlin GL., Sell SA (2014). Platelet-rich plasma in bone regeneration: Engineering the delivery for improved clinical efficacy. BioMed Res. Int. 2014: 1-15. https://doi.org/10.1155/2014/392398

Rolls G (2010). Microtomy and Paraffin Section Preparation. Scientia Leica Microsystems' Education Series. Series 32. https://www.leica-microsystems.com

Shibuya N, Jupiter DC (2015). Bone Graft Substitute: Allograft and Xenograft. Clin. Podiat. Med. Surg. 32(1): 21–34. https://doi.org/10.1016/j.cpm.2014.09.011

Singh CK, Sarma KK, Kalita D, Deuri B, Nath PJ (2017). Review on Fracture, Dislocation and Neurological Affections in Animals between April 2011 to March 2013 around the Urban and Suburban Area of Guwahati, India. Int. J. Curr. Microbiol. Appl. Sci. *6*(7): 1540–1550. https://doi.

org/10.20546/ijcmas.2017.607.184

Venkatesan J, Kim SK (2010). Effect of temperature on isolation and characterization of hydroxyapatite from tuna (thunnus obesus) bone. Materials. 3(10): 4761–4772. https://doi.org/10.3390/ma3104761

Veronese N, Maggi S (2018). Epidemiology and social costs of hip fracture. Injury. 49(8): 1458–1460. https://doi.org/10.1016/j.injury.2018.04.015

Wu A.-M., Bisignano C., James S. L., Abady G. G., Abedi A., Abu-Gharbieh E., Alhassan R. K., Alipour V., Arabloo J., Asaad M., Asmare W. N., Awedew, A. F., Banach M., Banerjee S. K., Bijani A., Birhanu T. T. M., Bolla S. R., Cámera L. A., Chang J.-C., Vos T. (2021). Global, regional, and national burden of bone fractures in 204 countries and territories, 1990–2019: a systematic analysis from the Global Burden of Disease Study 2019. Lancet Healthy Longevit. 2(9): e580–e592. https://doi.org/10.1016/s2666-7568(21)00172-0

Yi H, Ur Rehman F, Zhao C, Liu B, He N (2016). Recent advances in nano scaffolds for bone repair. Bone Res. *4*(1): 1-11. https://doi.org/10.1038/boneres.2016.50